Chem Soc Rev

TUTORIAL REVIEW

View Article Online
View Journal | View Issue

Cite this: *Chem. Soc. Rev.*, 2015, **44**, 1053

Received 16th October 2014

DOI: 10.1039/c4cs00342j

www.rsc.org/csr

Molecules with a sense of logic: a progress report

Joakim Andréasson*[a] and Uwe Pischel*[b]

In this tutorial review, the most recent developments in the field of molecular logic and information processing are discussed. Special emphasis is given to the report of progress in the concatenation of molecular logic devices and switches, the design of memory systems working according to the principles of sequential logic, the mimicking of transistors, and the research on photochromic platforms with an unprecedented degree of functional integration. Furthermore, a series of achievements that add up to the conceptual diversity of molecular logic is introduced, such as the realization of highly complex and logically reversible Toffoli and Fredkin gates by the action of DNAzymes or the use of a multi-fluorophoric platform as a viable approach towards keypad lock functions.

Key learning points
(1) A general introduction to molecular logic and information processing.
(2) The development of the field over the last five years.
(3) Functional integration and reconfiguration.
(4) Approaches to solving the concatenation issue.
(5) Implementation of memory effects in molecular logic.

1. Introduction and scope of the review

Molecular logic is a continuously developing multidisciplinary field that is driven by the beguiling idea of processing information contained in photonic, electrochemical, and chemical signals with the help of molecules and their inherent chemical transformations. The application of the binary notation, zeros and ones, and the principles of Boolean language form the basic principles of this approach. Such thoughts were formulated in the pioneering works by Aviram and de Silva about 20 years ago.[1,2] The first reported molecular logic AND gate used protons and sodium ions as chemical inputs and fluorescence as optical output.[2] Since then, the complexity of the realized logic functions has steadily increased. In particular, fluorescent or photoswitchable systems and their excited-state processes (charge- or electron transfer, energy transfer, proton transfer) have been frequently employed in the rational design of molecular logic devices.[3–5] Notably, biomolecular approaches, including DNA computing, have been reviewed recently[6] and will not be covered in extended detail in this tutorial review.

Nowadays, two main directions of molecular logic can be identified in the current literature: (a) the implementation of complex logic operations in molecular building blocks with the aim to imitate functions that are essential to conventional semiconductor-based computing and (b) the application of logic principles for the realization of utility functions, such as drug delivery and pro-drug activation, medical diagnostics, and smart materials.[7] Both trends will be addressed in this work. With respect to point (a) and for a realistic positioning of the field, it is necessary to point out clearly that a molecular computer that could in some way substitute current conventional computing is still just an ambitious future vision. Some of the obstacles on the way to this goal will be identified herein. However, the intellectual exercise of designing molecular systems that perform a desired logic function has already paved the way to thinking "outside-of-the-box" and given rise to a steadily growing number of useful molecular logic applications.

Where are the advantages of using molecules as logic devices? Besides their obvious small size and the potential of being organized into nanometric supramolecular assemblies, they rely most often on functional integration. In conventional circuitry, the corresponding logic gates have to be physically wired. However, molecules can simply integrate the function

[a] *Department of Chemical and Biological Engineering, Physical Chemistry, Chalmers University of Technology, SE-412 96 Göteborg, Sweden. E-mail: a-son@chalmers.se; Fax: +46 31 772 38 58; Tel: +46 31 772 28 38*
[b] *CIQSO – Centre for Research in Sustainable Chemistry and Department of Chemical Engineering, Physical Chemistry, and Organic Chemistry, University of Huelva, Campus de El Carmen s/n, E-21071 Huelva, Spain. E-mail: uwe.pischel@diq.uhu.es; Fax: +34 959 21 99 83; Tel: +34 959 21 99 82*

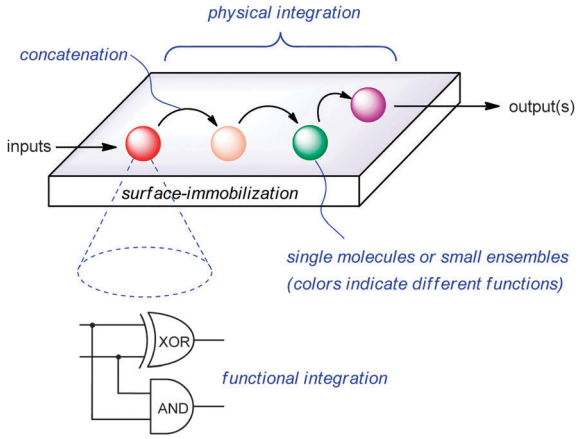

Fig. 1 Current challenges in molecular logic.

without presenting the implied gates by individual molecular entities. Another advantage is the often easily achieved reconfiguration by a flexible variation of the input and/or output reading. A *par excellence* example for the fantastic possibilities that these distinctive features (functional integration and reconfiguration) offer will be discussed herein for a multiphotochromic triad that enables the demonstration of no less than 14 (!) different logic operations.[8]

However, although functional integration can lead to the demonstrated high levels of complexity in unimolecular systems, the communication between various molecules, for example in supramolecular assemblies, is indispensable for the construction of molecular computers. Other questions that are of importance for molecular computing include the organization of molecular logic devices on surfaces and the demonstration of logic functionality for single molecules or small ensembles of molecules. Possible solutions for some of the herein outlined problems, which are summarized in Fig. 1, will be presented in this tutorial review.

The topics and examples that will be discussed in the following subchapters are mostly related to research that has been reported after the publication of our preceding overview in this journal in 2010.[4] Hence, the present work is meant to serve as a progress and status report that illustrates the further diversification of the field and the need to find solutions for the problems that are in sight.

2. Concatenation of logic gates

As outlined above, the concatenation of molecular logic gates and circuits is a current problem of molecular logic that imposes a bottleneck for further advancement of the field. Consequently, this question has started to draw increasing attention out of which some first proof-of-principle reports have appeared in the very recent literature.

The most common situation for a molecular logic gate comprises chemical input signals and optical outputs (very often fluorescence). This derives from the close conceptual relationship with chemosensing. The main obstacle for the concatenation of several such logic gates is that the signal heterogeneity would make it necessary to transform the optical output into a chemical species before it can be fed into the next molecular logic gate. Additionally, the multidirectional nature of emitted photons and the generally low intensity of fluorescence light are further limitations for using these photons efficiently in an intermediary photochemical process that could generate some sort of chemical species. However, some interesting approaches with focus on logic gates that build on communication *via* photonic or chemical signals have been reported in recent years and are discussed in the following paragraphs.

The implementation of logic operations with enzymatic systems has drawn much attention and was demonstrated in numerous examples from the groups of Katz and Willner. Enzymatic logic gates often consist of the substrates as chemical

Joakim Andréasson

Joakim Andréasson (born 1973) received his PhD from Chalmers University of Technology in 2002. After two years as a postdoctoral research fellow at Arizona State University, he returned to Chalmers to start up his own research group. He was appointed Assistant Professor in 2006, Associate Professor in 2008, and Professor in 2013. His research focuses primarily on molecular photoswitches and their potential applications in molecular information processing and optopharmacology.

Uwe Pischel

Uwe Pischel (born 1973) obtained his PhD in photochemistry from the University of Basel in 2001. After a postdoctoral stay at the Technical University of Valencia and independent stays at the University of Porto and the Technical University of Valencia he moved to the University of Huelva. He was appointed Assistant Professor in 2009 and Associate Professor at the end of 2012. He is the recipient of the Albert-Weller Prize of the German Chemical Society, the Ramón y Cajal Fellowship, and the Grammaticakis-Neumann Prize of the Swiss Chemical Society. His research focuses on molecular logic and switches, supramolecular host–guest chemistry, and fluorescent probes.

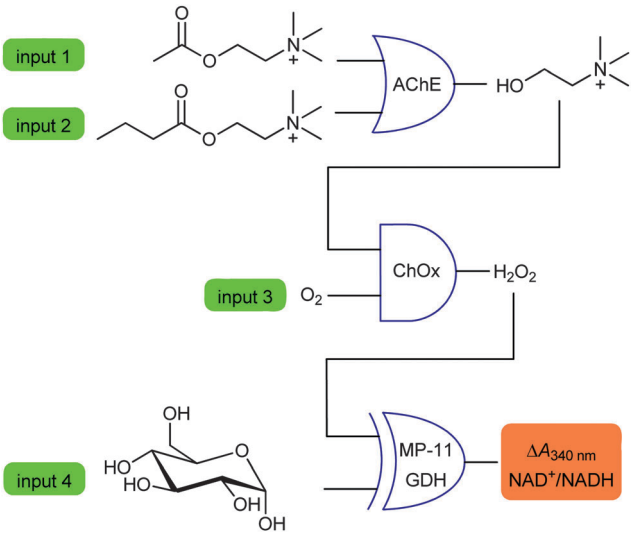

Fig. 2 Chemical concatenation of enzymatic logic gates.

inputs, the biocatalyst itself as the information processing unit, and the products as chemical outputs. By cleverly combining biocatalysts that rely on substrates that are the products of preceding enzymatic transformations, a cascade of concatenated enzymatic logic gates can be designed. In 2006, the Willner group reported such an example in which four biocatalysts are coupled [acetylcholine esterase (AChE), choline oxidase (ChOx), microperoxidase-11 (MP-11), and glucose dehydrogenase (GDH); see Fig. 2].[9] Acetylcholine and butyrylcholine are chosen as inputs 1 and 2 for AChE, respectively. Either of them gives choline as the output product corresponding to an OR operation. The choline is used as the input for the next logic gate that is operated by ChOx. Together with oxygen (input 3) this AND gate produces H_2O_2, which serves as the input for MP-11. The latter biocatalyst and GDH are linked by NAD^+/NADH as cofactors. While the presence of H_2O_2 (output of the preceding AND gate) yields NAD^+ formation, the addition of glucose (input 4) as substrate for GDH leads to NADH production (in absence of H_2O_2). The simultaneous presence of H_2O_2 and glucose counterbalances the antagonistic oxidation–reduction processes, and no net change in the NAD^+/NADH ratio is seen. The same applies for the "do nothing situation" (absence of H_2O_2 and glucose). By reading the modulus of the NADH absorption at 340 nm ($|\Delta A_{340}|$) as output, an XOR gate results. Effectively three logic gates, OR, AND, and XOR, are concatenated. While the enzymatic information processing units are recovered in their inherent catalytic cycles, the involved transformations lead to "waste" products. In principle, one could imagine ways to re-transform them into the initial substrates, which however was not attempted. The utility of such systems, being embedded in a bio-inspired context, is seen in "diagnostic computers" with the potential to follow on metabolic pathways or drug interactions.

The chemical signals that are used for the gate-to-gate communication can be also produced in photochemical transformations as shown in a recent work by the Akkaya group (see Fig. 3).[10] They used the photosensitizing capacity of Bodipy dyes to produce singlet oxygen ($^1O_2$). These dyes can be designed to permit the production of this reactive oxygen species in a

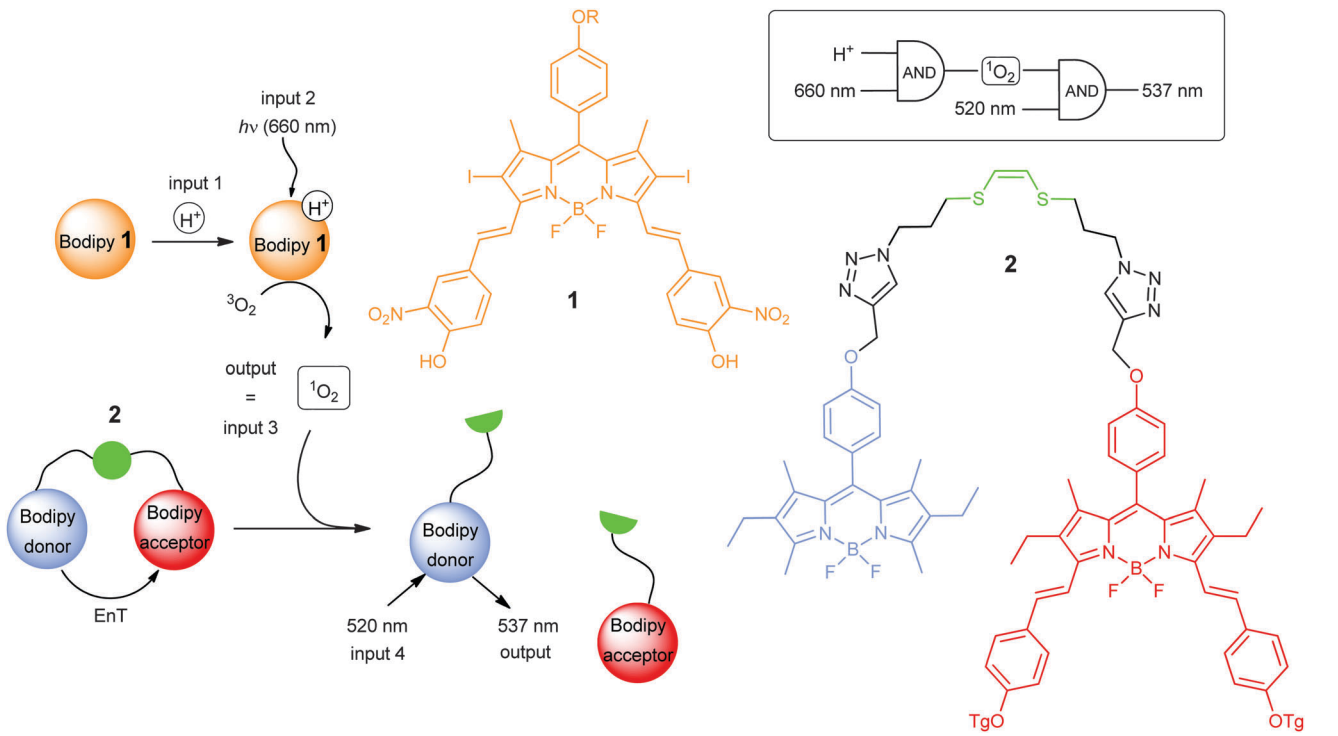

Fig. 3 Concatenation of logic AND gates by singlet oxygen formation and consumption (Tg: methoxytriethyleneglycol). Adapted from ref. 10 with permission from Wiley.

logically-controlled manner.[11,12] In the present system (Fig. 3), the two inputs are defined by light irradiation (660 nm) and pH. Dye **1** is designed such that the photosensitization is observed under acidic conditions but not for neutral or alkaline pH. Hence, the addition of protons (input 1) and irradiation with light (input 2) enables the production of $^1O_2$ according to AND logic. The $^1O_2$ output is used to activate another concatenated logic gate, the Bodipy-quencher dyad **2**. This system is designed to feature a Bodipy dye whose fluorescence is quenched by energy transfer (EnT) to an acceptor moiety (another Bodipy dye with a

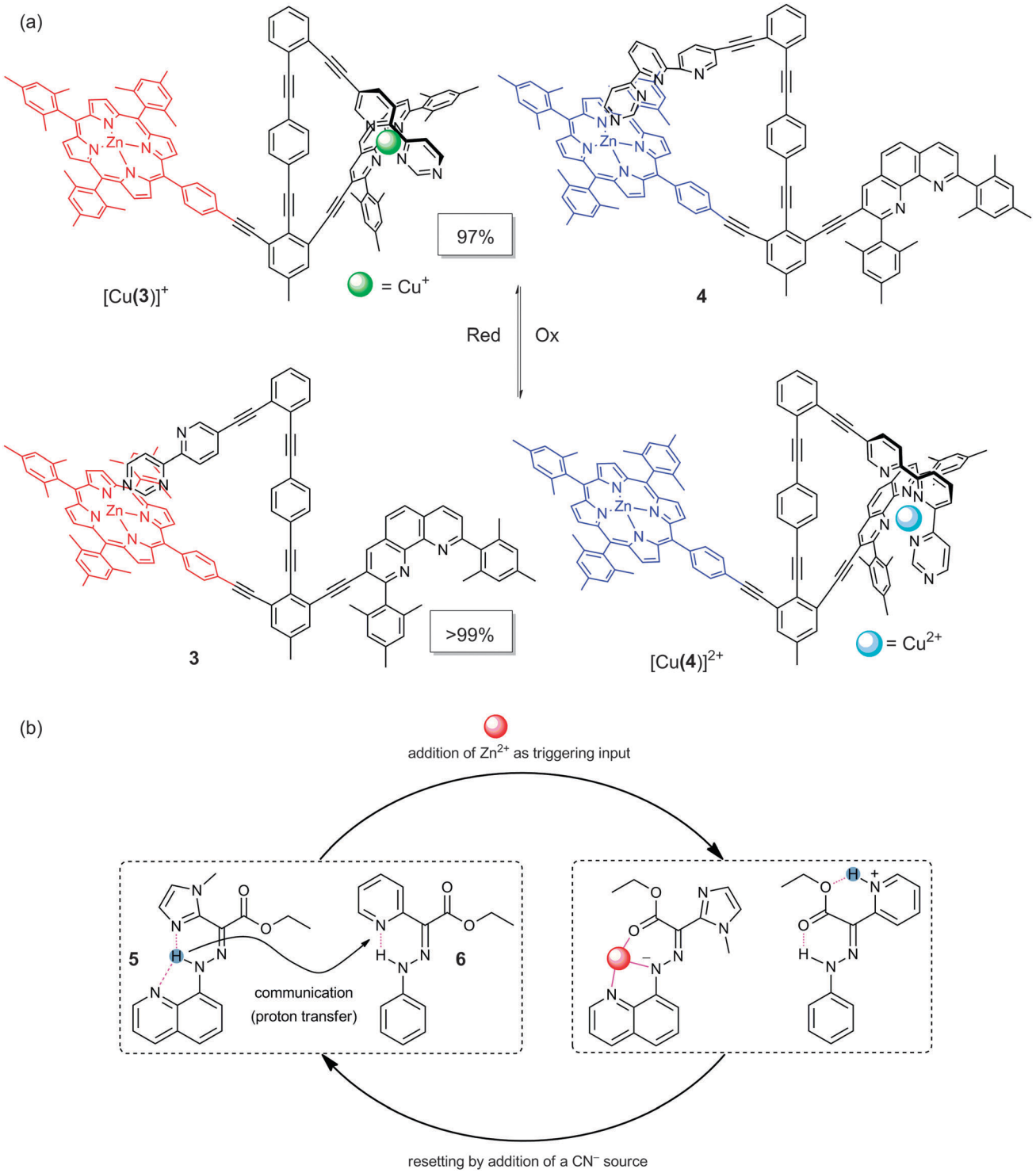

Fig. 4 Switch-to-switch communication by (a) redox chemistry and (b) coordination-coupled deprotonation. (a) was adapted from ref. 13 with permission from Wiley.

bathochromically shifted absorption) that is attached through a linker. The linker contains a (*Z*)-1,2-bis(alkylthio)ethene motif that can be efficiently cleaved by a reaction with the $^1O_2$ that is produced by dye **1**. The ultimate consequence is that the energy transfer is deactivated and fluorescence at 537 nm is detected upon excitation of the donor dye at 520 nm (input 3). In this way, two AND gates are chemically concatenated by the formation/consumption of $^1O_2$. Instead, using singlet-oxygen-scavenging glutathione as input 4, a concatenated INHIBIT gate is obtained. The role of $^1O_2$ as an agent in photodynamic cancer therapy as well as the role of slightly acidic pH and elevated glutathione levels as tumor-specific analytical parameters place this work into a scenario with potential clinical relevance.

Other works that use chemical signaling to enable communication between switches, but not necessarily with the background of logic operations, have been published in recent years (see Fig. 4). Schmittel and co-workers demonstrated the fast communication (timescale of few minutes) of two nanoswitches (**3** and **4**), which is triggered by electrochemical (or chemical) oxidation of Cu^+ to Cu^{2+}. This is followed by the release of the oxidized cation and its capture by a second nanoswitch.[13] They also showed that this may be extended to the communication between three switches.[14] Interestingly, the communication process is accompanied by pronounced geometrical changes in both switches, integrating the behavior of molecular machines. The reversibility of the redox chemistry allows recycling and thereby enables bidirectional signal communication. An example in which both the triggering input and communication signal are composed of chemical species was given by the Aprahamian group.[15] They employed the concept of coordination-coupled deprotonation to effectuate the transfer of a proton to compound **6** by the addition of Zn^{2+} to switch **5** (Fig. 4). This can be monitored by UV-vis and NMR spectroscopy. The process can be inverted by sequestering Zn^{2+} with cyanide ions. Other approaches used the proton release upon light-induced switching of a photochromic spiropyran to address luminescent pH-sensitive Ru^{2+} complexes or supramolecular host–guest complex formation.[16,17] To this point, the use of a chemical signal for the communication between two switches or logic devices was discussed. Indeed, already low or even catalytic concentrations of chemical output species may be enough to address concatenated switches. However, chemical cross reactivity could be an issue for systems that are more complex than the ones described herein as proof-of-principle examples.

The field of molecular logic was always strongly driven by the exploitation of photochemical or photophysical processes. The idea to enable the communication of molecular devices *via* a photophysical pathway such as EnT is a consequence of this driving force. Recently, the Akkaya group conducted a proof-of-principle experiment to demonstrate the EnT-concatenation of two logically-functional Bodipy dyes that are integrated in the dyad **7** (Fig. 5).[18] Effectively, two AND gates are communicated with the first one using light excitation (560 nm) AND Hg^{2+} ions as inputs and the second one run *via* EnT sensitization AND Zn^{2+} ions as inputs. Different fluorescence deactivation pathways are switched off by the metal ion inputs [ICT – intramolecular charge transfer (Hg^{2+}) and PET – photoinduced electron transfer (Zn^{2+})]. This enables EnT or the observation of the final fluorescence output (at 660 nm). By employing a Zn^{2+}-complex with a photocleavable ligand, a third logic gate (INHIBIT) can be added to this construct in which the photolysis light (360 nm) and Zn^{2+}-sequestering EDTA are the inputs.[19] However, the irreversible nature of the Zn^{2+}-releasing photoreaction is problematic for resetting and recycling without adding new chemicals.

EnT is a conceptually neat idea to concatenate switches and more specifically logic gates. It removes the multidirectional nature of fluorescence light that would apply in the case of the trivial and less efficient emission/re-absorption mechanism. In addition, this strategy allows for directional guidance of the photonic energy between logic gates. However, on the downside, the preparation of such multichromophoric arrays requires increased synthetic labor and the photophysical condition of selective excitation of the energy donor turns out to be more complicated with an increasing number of chromophores. The greatest obstacle is, however, that the successive EnT processes follow a thermodynamic downhill path, such that the number of concatenation steps is naturally limited.

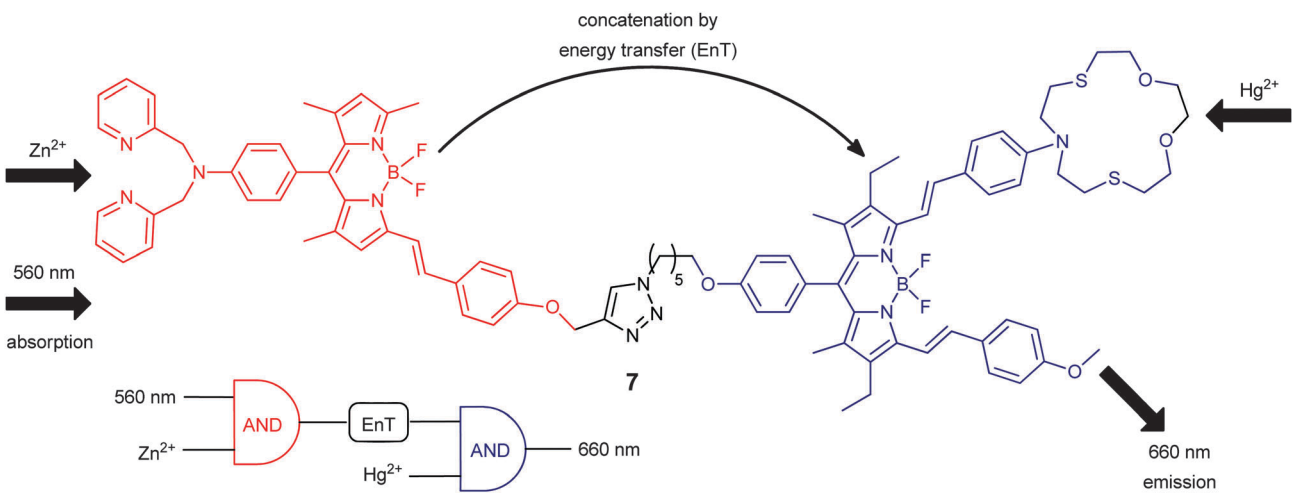

Fig. 5 Concatenation of two Bodipy-based molecular logic AND gates by energy transfer.

Very recently, the Schiller group came up with a completely different way of thinking about how to concatenate logic gates. Their approach builds on a network of IMPLICATION and FALSE gates that can be used to demonstrate any other logic operation.[20] They exploit their sugar-based IMPLICATION logic gate shown in Fig. 6.[20] The signaling system is presented using the widely employed fluorescent dye, 8-hydroxypyrene-1,3,6-trisulfonic acid trisodium salt (HPTS, **8**), and the inputs are constituted by a boronic acid-appended bipyridinium salt (**9**) and a diol-containing substrate (*e.g.*, fructose). On the one hand, the inherently high fluorescence of dye **8** is quenched by charge transfer in the complex **8**·**9**. On the other hand, the presence of only diol substrate leaves the fluorescence of **8** unaffected. However, the simultaneous presence of **9** and the diol leads to significant charge neutralization in the formed boronate ester and results in free fluorescent dye **8** rather than the weakly fluorescent complex **8**·**9**. As an ultimate consequence, this translates into an IMPLICATION gate. Here, the fluorescence output of **8** is always high (binary 1) except in the presence of **9** as the only input, leading to fluorescence quenching (output is assigned a binary 0; see truth table in Fig. 6). Notably, the same chemical principle, substituting the pyrene dye for a more light-stable perylene bisimide dye and using saccharide as the sugar input, was applied for the demonstration of the IMPLICATION operation at the single-molecule level.[21] The concatenation of several gates that rely on chemical inputs and fluorescence outputs suffers from the already described problem of input/output heterogeneity. The authors overcame this obstacle by applying an algorithm-based pipetting protocol in which the user translates the fluorescence output into the addition or no addition of the chemical inputs (**9** and fructose as diol-containing compound). Microtiter plates are used in order to achieve spatial compartmentalization. In Fig. 7, this procedure is sketched for the demonstration of an AND gate that is constructed from three IMPLICATION gates and two FALSE gates. Two binary inputs k and m are processed (presented in columns 1 and 2, respectively). The inverted input of the IMPLICATION gate is presented by the addition of **9**, while the other input is either 0 (represented by a FALSE function, meaning "do nothing") or the addition of fructose. At the beginning, all wells of the microtiter plate are loaded with **8** (high fluorescence). In step 1, the m input is applied to the red gate: $m = 1$ means addition of **9** to column 3, and $m = 0$ means no addition. The fluorescence output in column 3 is the output of the first (red) IMPLICATION gate. In step 2, the k input is applied to the green gate in the same way as accomplished for the m input (addition of **9** to column 4 for $k = 1$ and no addition for $k = 0$). The other input of the green gate, which at the same time is the output of the red gate (column 2) is represented by the corresponding addition of fructose to the wells in column 4. The superposition of both inputs (**9** and fructose) leads to the fluorescence output of the green gate, shown in column 4. In step 3, this output is translated into the addition of **9** to the wells in column 5, leading to the output of an AND gate with the inputs k and m. This approach can be extended and was used by the authors for the demonstration of a four-bit adder. This device comprises one half adder (combination of AND and XOR gate) and three full adders (combination of two XOR gates, two AND gates, and one OR gate). All implied elementary gates can be represented by networks of IMPLICATION and FALSE gates in similar ways as discussed above for the specific case of an AND gate.

However, despite several promising proof-of-principle demonstrations, the concatenation of logic gates continues to

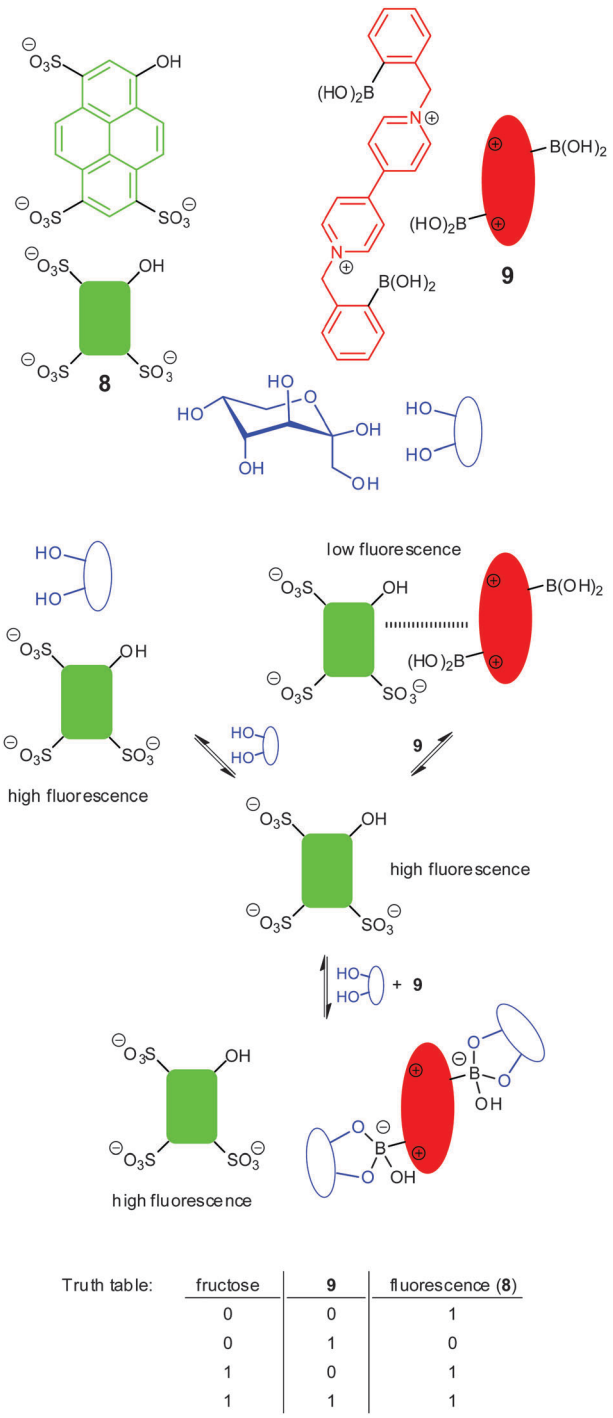

Truth table:

fructose	9	fluorescence (8)
0	0	1
0	1	0
1	0	1
1	1	1

Fig. 6 Chemical principles of the sugar computer and the IMPLICATION truth table. Adapted from ref. 20 with permission from Wiley.

be the bottleneck for the successful implementation of molecular logic. Further clever approaches are expected to appear in the coming years.

3. Memory effects in molecular systems

In the examples of molecular logic gates that were discussed so far in this tutorial review, the order of input application does not play a role; a typical observation for combinational logic. In computing applications of molecular logic, the implementation of memory is very desired, opening new dimensions for the storage and molecular-scale processing of information. Devices with memory deliver the output in function of the input history, being also called sequential logic devices.

In silicon circuitry, these operations are found in flip-flops. For example, a set–reset flip-flop is a bistable device that is characterized by a Q state that takes a value of 0 or 1. The flip-flop is fed by two inputs: set (S) and reset (R). Starting with the switch in state 0 ($Q_{current} = 0$) the application of the S input ($S = 1$) sets the Q state to $Q_{next} = 1$. From here, the device can be reset by input $R = 1$ back to the 0 state. Application of the S input over the already to $Q = 1$ set system leads to no further change. The same applies for $R = 1$, with the system being already in the $Q = 0$ state. Finally, the trivial doing nothing ($S = R = 0$) condition leaves the switch in its hold state. This observation manifests the memory function. Setting and resetting simultaneously ($S = R = 1$) has no physical meaning and is an undefined situation. Having made clear these general considerations in set–reset flip-flops, the specific chemical requirements for molecular systems are obvious:[22]

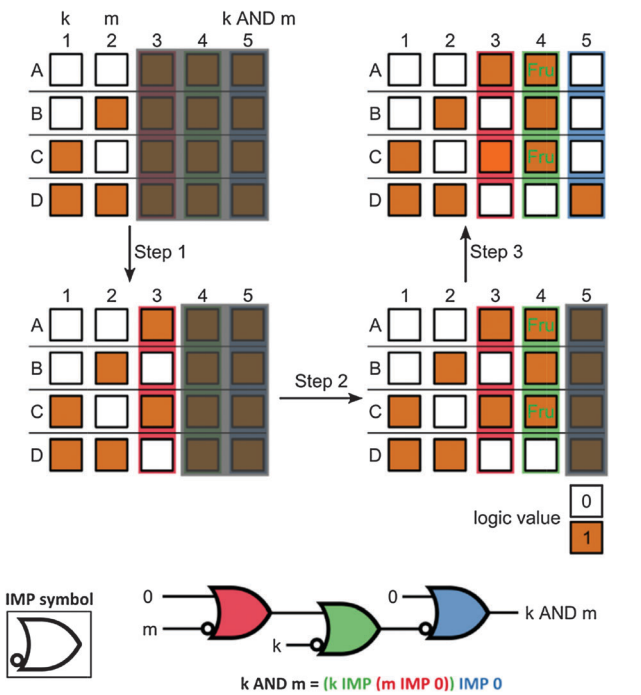

Fig. 7 Algorithm-based titration protocol for the concatenation of molecular IMPLICATION gates. Adapted from ref. 20 with permission from Wiley.

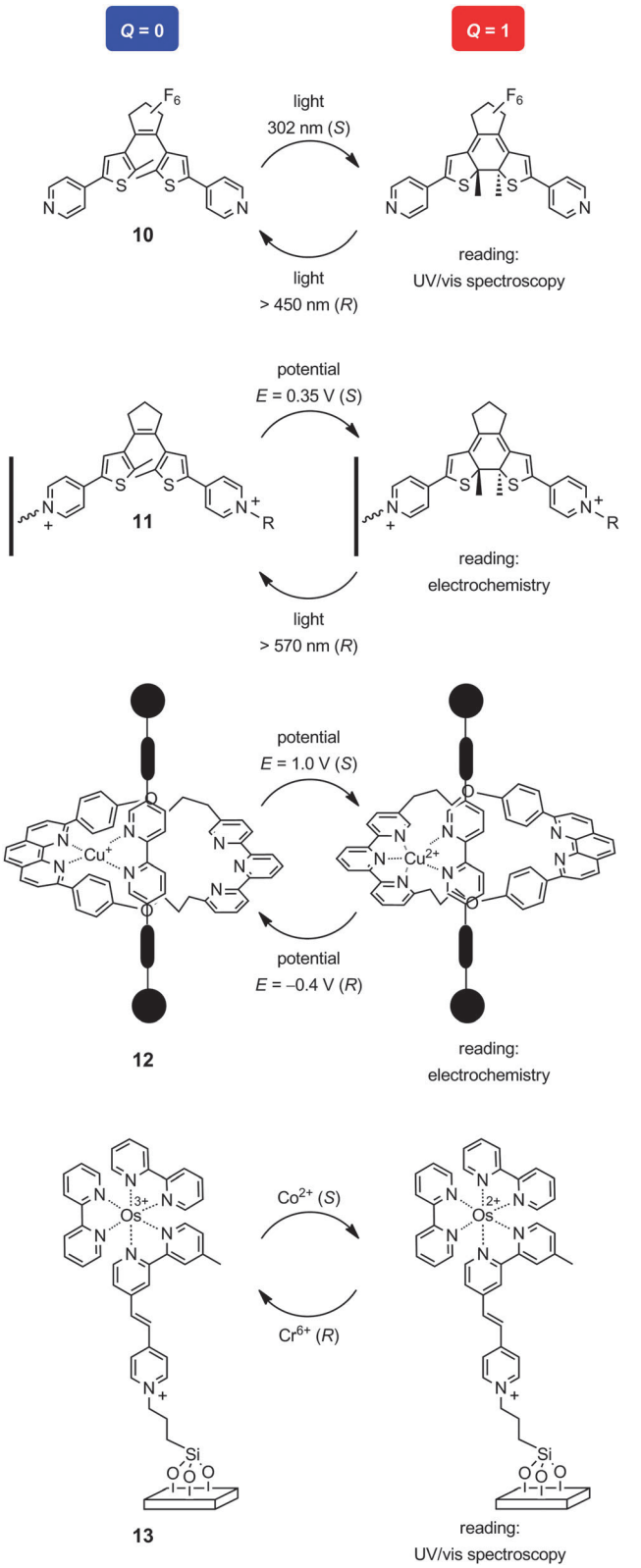

Fig. 8 Examples for molecular set–reset flip-flops.

• the molecular system has to feature two chemically stable forms with sufficiently differentiated physicochemical and easily readable properties (color, fluorescence, redox potentials, *etc.*),

• the conversion between both states should be efficient, clean, and reversible and the accumulation of input information (*e.g.*, input chemicals) should be avoided,

• the *S* and *R* inputs have to act state specifically; unselective stimuli or chemical cross talk have to be excluded.

These preconditions have been shown to be satisfied chemically by quite diverse systems (see examples **10–13** in Fig. 8). These can be addressed by chemical and electrochemical redox processes or by light irradiation.[22–25]

One of the examples, the Os^{2+} polypyridyl complex **13** with a trialkoxysilyl anchor for immobilization on a glass surface, was reported by the van der Boom group in 2010.[25] As the *S* input, the reducing agent Co^{2+} is chosen while the role of the *R* input is fulfilled by the oxidizing Cr^{6+}. The metal-to-ligand charge transfer (MLCT) absorption of the Os^{2+}-complex at 496 nm is read as the output. On the one hand, activating the *S* input sets the system to the Os^{2+} state (high output signal, $Q = 1$) or maintains it in this state. On the other hand, the addition of Cr^{6+}, which is compatible with $R = 1$, resets the flip-flop to the Os^{3+} state and thereby to $Q = 0$ or preserves this state. While in solution, the chemical inputs would accumulate with each set–reset cycle (10 stable cycles were experimentally demonstrated), and this is elegantly avoided by having the system surface-immobilized. This enables the removal of any excess input chemicals or the corresponding derived species by a simple "dip and wash" protocol. The retention time of the written information is given as a minimum of 10 minutes.

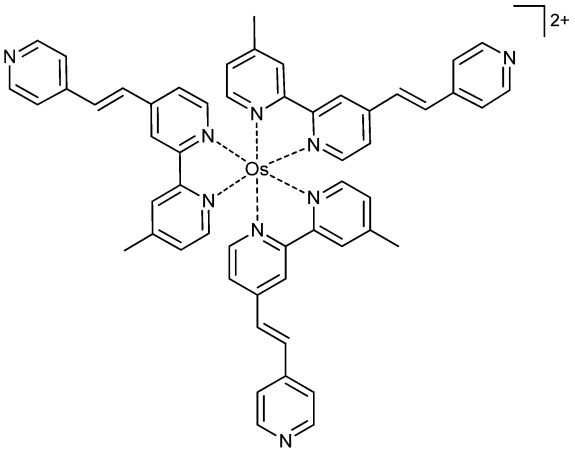

14

In an extension of this work, an electrochemically-addressable device that allows the writing and reading of multi-valued information, a flip-flap-flop, was presented by the van der Boom group.[26] While binary values are assigned to the above described bistable situation, a system with *n* stable states leads to *n*-valued logic. Hence, the tri-stable situation that is integrated by the flip-flap-flop can be described by low, medium, and high state values (corresponding to 0, 1, 2 or −1, 0, 1 as is also frequently used). In detail, the Os^{2+} complex **14** was applied as a precursor to grow a film by alternate deposition of this ligand and $PdCl_2$ on pyridyl-functionalized indium-tin-oxide (ITO)-coated glass. The set–reset cycle is triggered by electrical input potentials. By choosing adequate potentials (for full oxidation and reduction) a binary set–reset flip-flop is realized through reading of the MLCT absorption at 510 nm. The response time and recycling capability of this electrically addressable flip-flop are superior by various orders of magnitude as compared to those of the above described chemically triggered counterpart. Introducing a third input potential, by which neither full oxidation nor full reduction is achieved, enables the definition of three input and three output levels. This leads to the announced flip-flap-flop device. Notably, in this case, the ternary switching derives from the absorption signal integrated over all molecules of the macroscopic device. However, each individual molecule retains its binary behavior, existing in only two states. Multi-valued switching of individual molecular devices has been reported as well.[27,28]

In 2012 a collaboration between the groups of Credi and Stoddart resulted in the [2]rotaxane **15** (see Fig. 9) as a supramolecular memory device in which the retention time of the written data is controlled by a built-in photochemical locking mechanism.[29] First, only considering the two stations, a tetrathiafulvalene (TTF) and a 1,5-dioxynaphthalene (DNP) unit, the bistable system can be addressed in a thermodynamically controlled fashion by using the redox chemistry of the TTF station. In the initial state, the tetra-cationic ring component resides over the TTF station, which is signalized by a characteristic charge-transfer (CT) absorption band at *ca.* 850 nm. However, upon chemical oxidation of the TTF station with Fe^{3+} ions, the CT interactions are weakened and the ring dislocates to a second station (DNP). Upon reduction of the TTF radical cation with decamethylferrocene, the ring resides for a limited time on the DNP station before shuttling back to the stronger interacting neutral TTF station. At this point, the central photoisomerizable azobenzene comes into play. While the *trans* form constitutes no obstacle for the passing of the ring, the *cis* form installs a kinetic barrier. Hence, upon

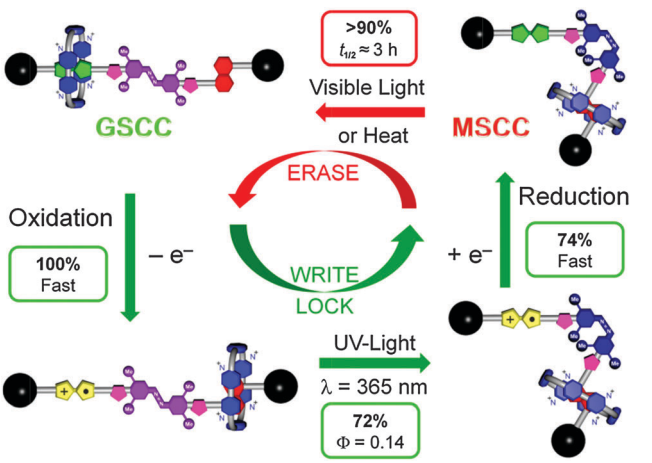

Fig. 9 Erase-write/lock cycle of rotaxane **15** (GSCC: ground state co-conformation; MSCC: meta-stable state co-conformation). Reproduced from ref. 29 with permission from Wiley.

trans–cis isomerization triggered by UV light (365 nm), the ring can be locked. In this case, the written information is conserved for a half life of *ca.* 3 hours, corresponding to the slow *cis–trans* thermal back isomerization. However, first applying the light input, isomerizing the azobenzene to the *cis* form and then oxidizing the TTF does not lead to the dislocation of the ring to the DNB station. This is indirectly evidenced by the hindered oxidation of the TTF. This indicates another interesting feature of the system: the photocontrolled protection against accidental writing. The memory effect of the rotaxane **15** is imposed by the phototriggered switching of the azobenzene unit.

The notion that photochromic switching is inherently connected to a memory effect was used by the Andréasson and Pischel groups to construct a D flip-flop (delay or data flip-flop).[30] For this purpose, the fulgimide derivative **16** was exploited (see Fig. 10). Fulgimides exist in two isomeric open forms (*E* and *Z*) that can be equilibrated by UV light irradiation and one closed form that is produced from the *E* form in a 6π electrocyclic reaction triggered by UV light (*e.g.*, 355 nm light). The reverse ring-opening reaction can be initiated by irradiation with visible light (*e.g.*, 532 nm light). The closed form is weakly fluorescent (*ca.* 640 nm). This can be used to read the state *Q* of the switch (*Q* = 0 means non-fluorescent and *Q* = 1 corresponds to the observation of fluorescence).

The D flip-flop has two inputs, a clock input (*Clk*) and a data input (*In*), which for our photochromic system are represented by light of different irradiation wavelengths. In the concrete case, the *Clk* input corresponds to 532 nm light, while 1064 nm light stands for the *In* input. Whenever the condition *Clk* = 0 is fulfilled, the system maintains its present state *Q* ($Q_{current}$ = Q_{next}). This means that the input *In* alone should do nothing to the system. Because **16** is thermally stable in all its forms, near-infrared irradiation leaves the system unchanged. On the other hand, when *Clk* = 1 the Q_{next} state corresponds to the value of the *In* input. Photochemically, this translates into a situation in which the sole application of the *Clk* input results in the non-fluorescent *Q* = 0 state. In accordance, the irradiation with 532 nm light sets the system to the non-fluorescent open *E* form. However, in conjugation with the photonic input corresponding to *In*, the reverse photoreaction should be triggered. This is a delicate and non-trivial problem that was approached with a nonlinear optical phenomenon: a third-harmonic-generator crystal generates 355 nm light when hit simultaneously by 1064 nm and 532 nm light beams. The UV light produces the closed fluorescent form, corresponding to *Q* = 1. All irradiation wavelengths were generated from the fundamental wavelength (1064 nm) of a Nd:YAG laser with the help of frequency multiplication. The all-photonic working mode of this molecular device overcomes at least formally the mentioned barrier of input/output heterogeneity.

Notably, other photochromic systems were used as molecular keypad locks that are also considered as sequential logic devices and in which the order of input application is decisive for the output (see Section 6 for a concrete example). This was already discussed in detail in our earlier tutorial review.[4] Since then, new examples based on photoswitches have been reported.[8,31,32] Another clever photochromic system that builds on the light-induced writing and erasing of information was reported by the groups of Zhu, Tian, and Li.[33] Here, the memory effect is expressed in the photomodulation of a white light input beam, enabling the encoding of optical signals.

A memory function in a biochemically activated system was reported by the Katz group. They devised an associative memory[34] based on cascades of enzymatic reactions, which are conceptually related to the ones discussed above in the context of bioinspired concatenation.[9] A concentration-optimized mixture of NAD^+, ATP, and maltose in phosphate buffered saline (pH 7) is addressed by several enzyme inputs (Fig. 11). The combination of maltose phosphorylase (MPh) and glucose dehydrogenase (GDH), denoted as "correct input", triggers the transformation sequence maltose → glucose → gluconic acid. This process is accompanied by the reduction of NAD^+ to NADH. The absorbance of the latter at 340 nm serves as an optical output reading. The other enzyme combination, named as "wrong input", consists of hexokinase (HK) and glucose-6-phosphate dehydrogenase (G6PDH) and does not trigger any reaction in the absence of glucose. However, by applying the "correct" and "wrong" enzyme inputs simultaneously, part of the glucose that was produced by the action of

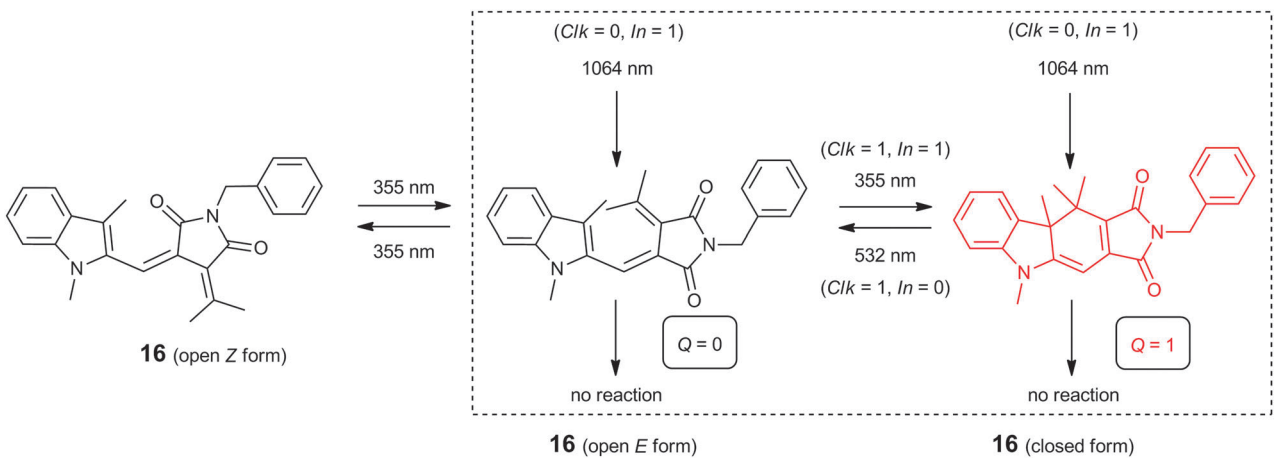

Fig. 10 Photochromic switching of fulgimide **16** for the realization of a D flip-flop.

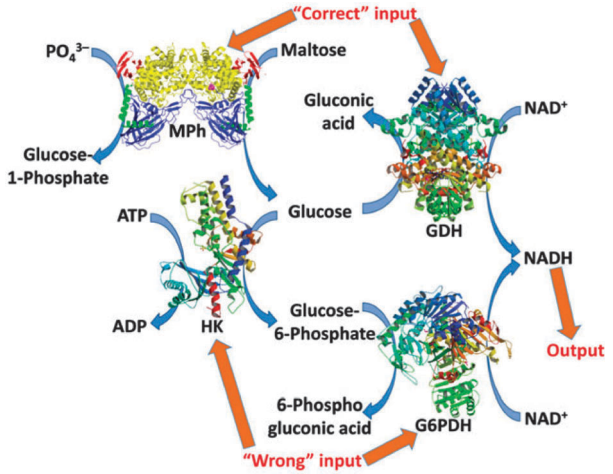

Fig. 11 Associative memory with an enzymatic logic system. Reproduced from ref. 34.

MPh is implicated in the HK-catalyzed formation of glucose-6-phosphate. This in turn leads to the G6PDH-catalyzed formation of NADH (see Fig. 11). By fine-tuning of the relative enzyme activities of HK and G6PDH, an accumulation of glucose-6-phosphate can be achieved. This serves as the memorized information and yields NADH output even in the case of the application of a "wrong" input. These "training" and "memory" characteristics of the system's activity define an associative memory that has been illustratively compared to Pavlov's dog experiments.

As can be seen, the expression of memory in molecular and supramolecular systems can be diverse. The control of these functionalities can be achieved chemically, electrochemically or photochemically. Despite the low storage capacity of the discussed systems, the level of complexity in terms of information processing is remarkable.

4. Systems with transistor-like responses

Transistors are the key players in today's electronic devices, including the silicon-based versions of the logic gates and all other circuits described above. This is, among other things, due to the ability of a transistor to switch between 0 and 1 with GHz frequency. The conventional transistor has typically three terminals, where the voltage between two terminals controls the *I–V* (current–voltage) characteristics between the other two terminals. However, as for all other molecule-based logic devices, the types of input and output information are not restricted to voltage. They may instead be represented by any other kind of signal. In this section, examples of molecular constructs with transistor-like behavior will be given, using cations, protons, and light as the external stimuli. In all cases and as in many of the systems that were discussed before, fluorescence emission serves as the conveniently detectable output.

Compound **17** (Fig. 12) was designed by de Silva and co-workers to display anthracene-based fluorescence sensitive to both pH and

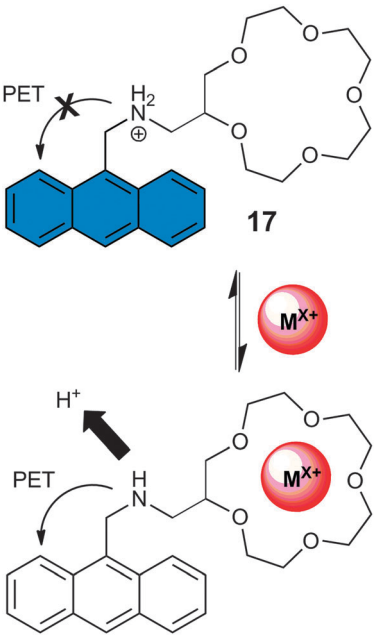

Fig. 12 pK_a-Shift and the resulting PET switching induced by cation complexation to the crown ether.

the presence of various cations.[35] The amine receptor efficiently quenches the anthracene emission by PET in its non-protonated form whereas this process is thermodynamically unfavorable upon protonation. Hence, the emission intensity is well described by the Henderson–Hasselbalch formulation, where the actual pH and the pK_a-value of the amine receptor determine the emission intensity. The neighboring crown ether serves as a receptor for metal cations. Due to electrostatic repulsion of the bound cations and the protonated amine, the system experiences a pK_a-shift upon the addition of metal ions. This shift is mainly dependent on the metal ion charge, leading thereby to a displacement of the fluorescence *vs.* pH titration curve dependent on the cation. Hence, this purely chemical phenomenon resembles transistor-like behavior where the analogous effect is seen in the *I–V* curves. Similar displacements of pH titration curves, albeit not interpreted in terms of a transistor analogy, were observed for competitive guest dye displacement from a cucurbituril macrocycle upon addition of sodium ions.[36]

Gust and co-workers used a photochromic hexad consisting of a dithienylethene (DTE) photoswitch and five bis(phenylethynyl)-anthracene (BPEA) fluorophores covalently linked to a benzene core (compound **18** in Fig. 13).[37] As indicated also in Fig. 8, DTE derivatives exist in open (DTEo) and closed (DTEc) isomeric forms that are interconverted by the use of UV and visible light. The accompanying absorption changes are dramatic, as DTEo displays absorption in the UV region only, whereas DTEc has strong absorption also in the visible region. This opens up the possibility to switch on and off the action of EnT between DTE and an appended chromophore with fluorescence emission only in the visible region. Exposing **18o** to 350 nm UV light induces BPEA-based fluorescence emission centered at around 515 nm with a quantum yield close to unity. No quenching by EnT is

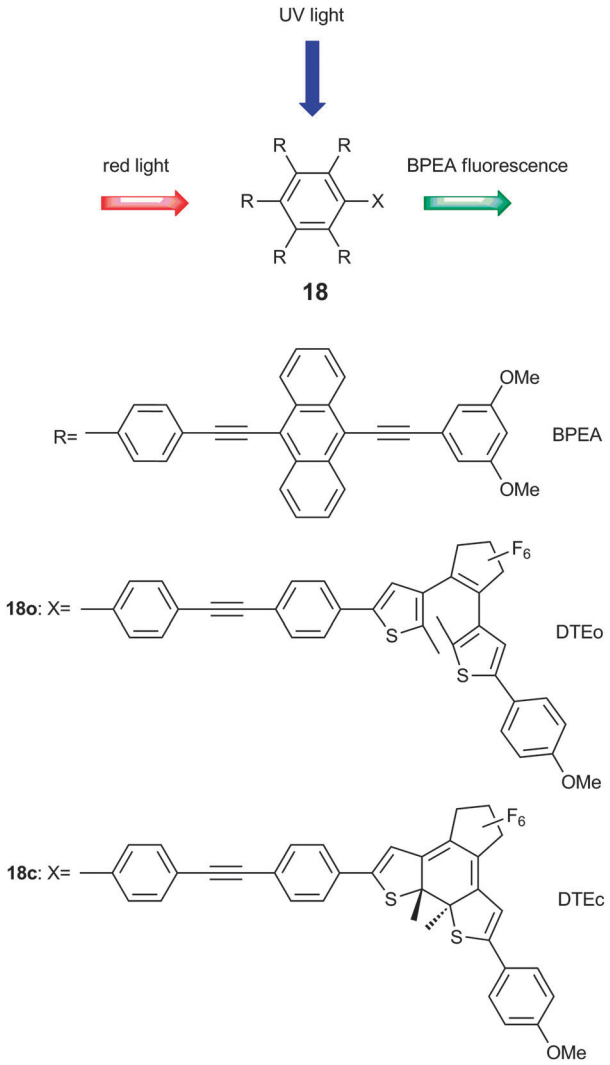

Fig. 13 Continuous intensity variations of the BPEA fluorescence stimulated by red light-induced isomerization of the DTE photoswitch.

initially observed, as there is no spectral overlap between the DTEo absorption and BPEA emission. With time, however, the 350 nm UV light triggers the isomerization **18o** → **18c**. In **18c**, the BPEA emission is quenched by DTEc in an efficient EnT process due to the significant spectral overlap between BPEA emission and DTEc absorption. In order to suppress this quenching process, **18c** can be exposed to red light at $\lambda >$ 610 nm, which triggers the reverse isomerization process **18c** → **18o**. This indicates that the relative concentrations of fluorescent **18o** and non-fluorescent **18c** are determined by the intensity of the red light (using a constant intensity of the 350 nm UV light). Hence, by modulating the flux of the red light, the BPEA-based fluorescence intensity at 515 nm varies accordingly. Not only does this behavior parallel that of a transistor, it is also an interesting example of the use of long-wavelength light to modulate the emission intensity at shorter wavelengths.

Köhler and co-workers designed a similar DTE-based photoswitchable molecule, aiming at an optical transistor (**19** in Fig. 14).[38] Here, two perylene bisimide (PBI) fluorescence reporter

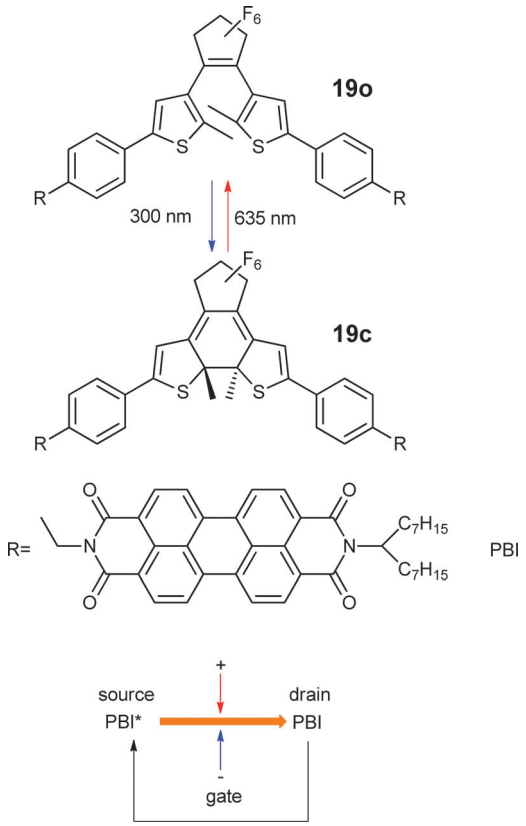

Fig. 14 Transistor-like variations in the PBI emission intensity through energy transfer switching.

units are flanking the central DTE photoswitch. As in the example mentioned above, the PBI fluorescence is quenched by DTEc in an EnT process. On the contrary, unquenched and intense emission is observed when the photoswitch is in the DTEo isomeric form. The inputs for this construct are UV light at 300 nm and visible light at 635 nm. Exposure to a fixed flux of 635 nm light (triggering the conversion to the fluorescent isomer **19o**) together with UV light of varying intensity (triggering the conversion to the non-fluorescent isomer **19c**) allows for fine tuning of the ratio [**19o**]/[**19c**]. This in turn leads to changes in the PBI emission intensity. Here, an increased UV intensity decreases the emission intensity. In the inverted version of this scheme, the UV flux was kept constant, whereas the intensity of the 635 nm light was varied. The PBI emission intensity-variations with the tuned light source are now reversed: an increased intensity of the 635 nm light increases the emission intensity. In the operation of this construct, the relative variation in PBI emission intensity was used as the output. With the 300 nm and the 635 nm "conversion beams" corresponding to the gate voltage polarity of a conventional transistor according to Fig. 14, the function of an optical version is described.

5. Functional integration in multi-switchable platforms

As discussed in the Introduction, functional integration and reconfiguration are key properties of molecular devices that are

typically not shared by the conventional silicon-based circuits. Although the field of molecular logic and information processing has indeed been brought forward by 20 years of collective effort from the research community, functional integration and reconfiguration must be considered as the main drivers. As an example, in the paradigm study by de Silva in 1993, an anthracene-based fluorescence reporter equipped with two receptors is operated with Na^+ and protons as inputs. Monitoring the fluorescence intensity from the anthracene reporter as a function of the input combinations allowed for the realization of a molecular AND gate.[2] This should be contrasted to the state-of-the-art examples, in which several properties (used as outputs) are altered by a large number of stimuli. Among these are chemical, electrochemical, and photonic signals that enable a molecular species to perform a multitude of logic functions.

A recent example along these lines was reported by Andréasson, Pischel, and Gust. Here, a molecular triad consisting of fulgimide (FG) and DTE photoswitches (**20** in Fig. 15) was used as the molecular platform.[8] By carefully selecting the wavelengths used for isomerization purposes, the FG and the DTE units could be selectively addressed as for the isomerization reactions. This allows for high enrichment of all four isomeric forms of the triad: FGo–DTEo, FGc–DTEo, FGo–DTEc, and FGc–DTEc, as depicted in Fig. 15. Each of these forms offers unique signatures in the UV-vis absorption spectra. In addition, the isomer-specific intramolecular communication in the excited state allows for controlling EnT processes, which in turn results in useful variations of the emission intensity. Altogether, these spectral features constitute the set of output signals used in the operation. For example, the only fluorescent form is FGc–DTEo. This is due to the fluorescent nature of FGc, in combination with the fact that DTEo does not quench the fluorescence by EnT, whereas DTEc does so. By the use of six photonic inputs (302 nm, 366 nm, 380 nm, 397 nm, green light, and red light) and output readings at five different wavelengths, no less than 14 logic functions are described. These include combinational-, sequential-, and reversible logic operations. In Section 6, the operation of this molecular construct as a parity generator/checker will be described in detail.[39] Besides the elevated level of functional integration, it should be stressed that the system works in the all-photonic mode of operation, *i.e.*, it draws exclusively on optical input and output signals.[40] This bypasses at least formally the abovementioned input/output heterogeneity, although in practical terms, no switch-to-switch communication has been reported for this system yet. Another surplus is the strict reversibility of the photochromic processes combined with a reasonable to high fatigue resistance. The initial state (FGo–DTEo) can be reached from any other state of the switch by irradiation with green light. This guarantees a resettable operation with increased recycling capability.

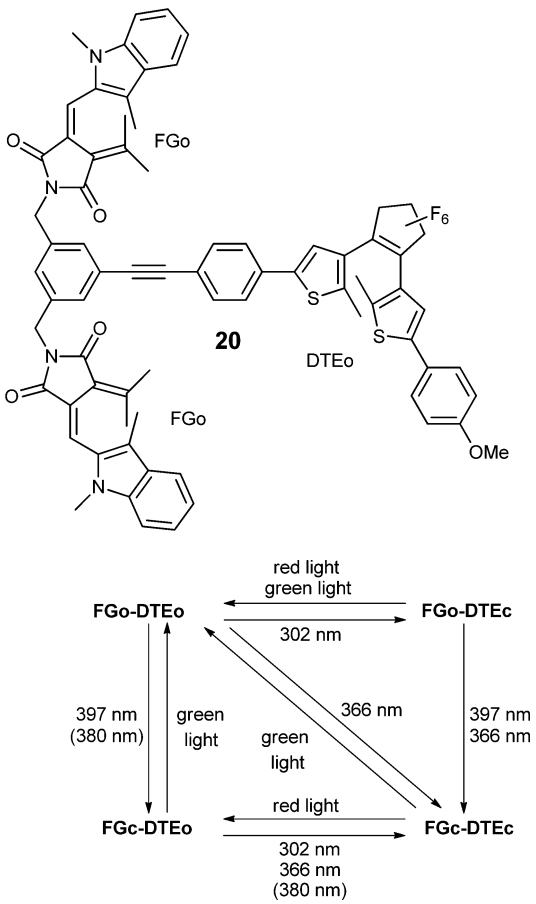

Fig. 15 Structure of the all-open isomeric form of the FG-DTE multitasking triad **20** (top) together with the corresponding isomerization scheme (bottom).

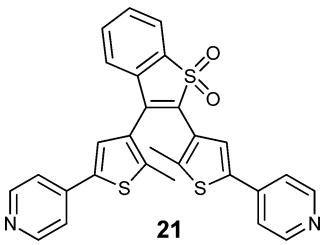

The groups of Tian and Zhu presented a multi-addressable terarylene-based photoswitch (BTO, **21**) appended with pyridine units that coordinate both Hg^{2+} and Cu^{2+} ions.[41] In combination with protons and UV light, these cations constitute the set of input signals. UV light is triggering the isomerization process from the open form of **21** (referred to herein as **21o**) to the corresponding closed form, **21c**. This process is fully reversed by visible light exposure. The addition of protons, Hg^{2+}, and Cu^{2+} each induces significant absorption changes for both **21o** and **21c**. Thereby, rich opportunities to devise input combinations and their respective outputs are provided (half adder, half subtractor, 4 : 2 encoder, 2 : 4 decoder, and the 1 : 2 demultiplexer). For example, UV irradiation of **21o** to form **21c** results in high absorption at 370 nm. This is true also for the situation when Hg^{2+} is added to **21o** to form the **21o**–Hg^{2+} complex. However, the absorption spectrum of **21c**–Hg^{2+}, formed upon UV exposure together with the addition of Hg^{2+}, does not display this distinctive band at 370 nm. Instead, **21c**–Hg^{2+} has the strongest absorption at 640 nm. Hence, by monitoring the absorption at 370 nm and 640 nm, the functions of a XOR gate and an AND gate are mimicked, respectively.

The parallel operation of these two logic gates results in a half adder that is able to sum up two binary digits.

These two examples define certainly the current state-of the-art in functional integration and demonstrate the elevated level of complexity that can be introduced by this powerful approach. Chemically, both systems build on either the combination of various independently addressable photochromic switches or the combination of photochromic processes with multiple chemical inputs. This leads to a multitude of input combinations that generate various well-differentiated optical output fingerprints.

6. New tools in the toolbox or thinking out of the box

As described in our tutorial review from 2010, the research front at that time was at a stage where molecular versions of the half adder and half subtractor together with their full versions were devised by several groups.[4] Reports on keypad locks, encoders/decoders and multiplexers/demultiplexers were just starting to emerge, later including surface-immobilized versions[42] as well. During the last five years, substantial effort has been put into the design of molecules capable of mimicking the function of additional electronic devices, frequently found in conventional hardware. We will begin this section by highlighting two such examples. This will be followed by the description of two supramolecular constructs with unprecedented sensing capability, and how the spectral responses are interpreted in terms of logic operations. Finally, the concept of fuzzy logic will be introduced and exemplified by a study in which a molecular photoswitch was used to mimic this extreme type of multi-valued switching.

Let us begin by reverting to the two-input–one-output logic gates. All 16 possible combinations of this kind are irreversible, meaning that all the applied input combinations cannot be traced back from the observed binary output. In other words, there are at least two input combinations that generate the same output, which implies that information is lost in the processing of the input vectors. Reversible logic operations, *i.e.*, where each input combination has its unique output, can be realized only by the use of additional output vectors. In this context, the two-input–two-output versions (*e.g.*, the Feynman gate) have been mimicked by the use of cleverly designed supramolecules.[31,43,44] Molecule-based versions of the three-input–three-output reversible logic gates, however, remained elusive until the recent report on Toffoli and Fredkin gates by the groups of Levine, Willner, and Remacle.[45] The truth table of the Toffoli gate example is shown in Table 1.

For the Toffoli gate, the states of inputs I_1 and I_2 are transferred directly to O_1 and O_2, respectively. This pairwise relation is true also for I_3 and O_3, unless both I_1 and I_2 are set to 1. In this case, O_3 is inverted with respect to I_3. For the Fredkin gate, the state of I_1 is always transferred to O_1. I_2 and I_3 are transferred to O_2 and O_3, respectively, when I_1 is 0. When I_1 is set to 1, however, I_2 is transferred to O_3, and I_3 is transferred to O_2. In other words, the Toffoli gate flips the third bit if the first two bits are 1, whereas the Fredkin gate swaps the last two bits if the first bit is 1. As for the ease of realizing the different rows in the truth tables by reading the input-dependent spectral responses of ''smart molecules'', it is easily seen for the example of the Toffoli gate that the entries 7 and 8 are the complex ones. All other entries simply represent a direct transfer of the inputs to the respective output and would be very straightforward to realize by the combination of three orthogonal one-input TRANSFER gates.

Table 1 Truth table for a Toffoli gate

	Inputs			Outputs		
Entry	I_1	I_2	I_3	O_1	O_2	O_3
1	0	0	0	0	0	0
2	0	0	1	0	0	1
3	0	1	0	0	1	0
4	0	1	1	0	1	1
5	1	0	0	1	0	0
6	1	0	1	1	0	1
7	1	1	0	1	1	1
8	1	1	1	1	1	0

Levine, Willner, Remacle and co-workers used a Mg^{2+}-dependent DNAzyme system in their biomolecular interpretations of the abovementioned reversible gates.[45] Notably a similar approach was successfully used for the demonstration of 2:1 and 4:1 multiplexers and a 1:2 demultiplexer in a follow-up work by the same groups.[46] As indicated in Fig. 16, the system used to mimic the behavior of the Toffoli gate consists of a library of eight single-stranded (SS) oligonucleotides. Three of these are each labeled with a fluorophore (F)–quencher (Q) (donor–acceptor) EnT pair at the 3′ and the 5′ ends. The three fluorophores (F_1, F_2, and F_3) have all distinct wavelengths of the emission maxima, *i.e.*, the intensities can be monitored separately and are used as the three outputs (O_1, O_2, and O_3). Moreover, the emission from F_1, F_2, and F_3 is quenched by Q, unless bulge-like DNAzyme structures are formed to induce cleavage of the F–Q-appended oligonucleotides (see I, II, III, and IV in Fig. 16). As inputs, three additional SS oligonucleotides were used. The nucleic acid sequences of the input strands are such that the DNAzyme structures, required to induce the fluorescence outputs of F_1, F_2, and F_3, are formed in a manner consistent with the truth table of the Toffoli gate (Table 1).

Although this system is reversible in logic terms, the operation is irreversible in the sense that it cannot be reset to the initial state (the situation before addition of the input strands). Instead, new material must replace the already used oligonucleotide library before the gates can be used to process new data. The use of all-photonic devices circumvents this obvious drawback, as photonic inputs leave no waste behind. Below is an example of this kind.

The photochromic triad **20** was described above as a multifunctional molecular platform capable of performing a multitude of logic operations.[8] One of these is the function of a parity generator/checker, an essential device in the detection of erroneous procedures in data transmission. The 2-bit parity

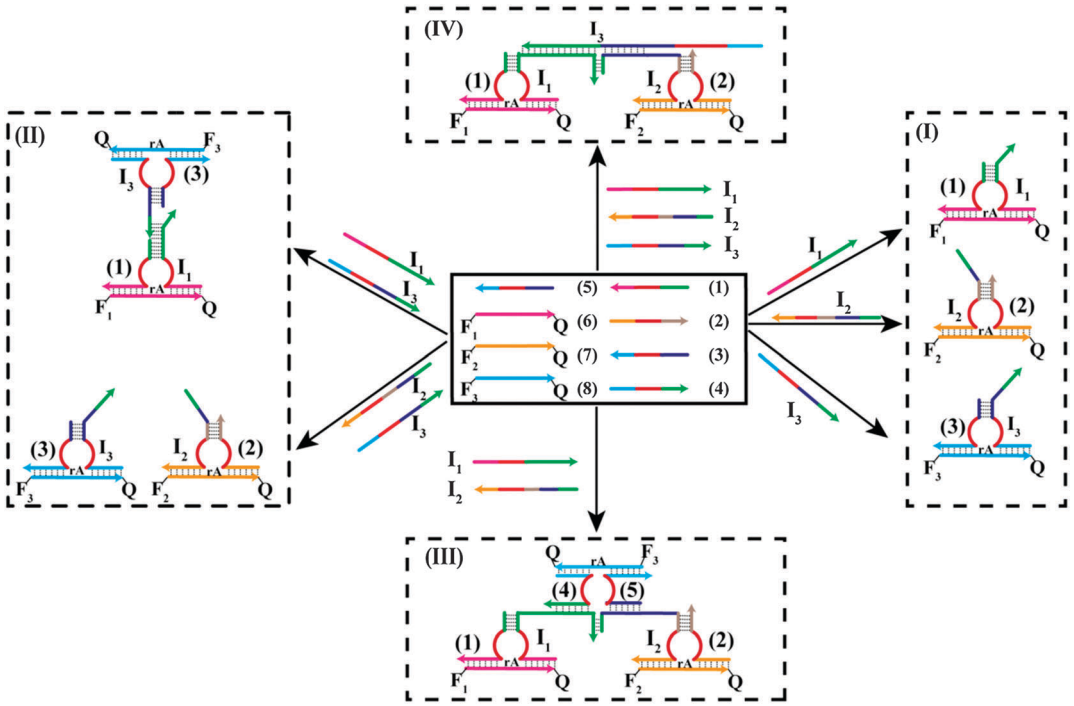

Fig. 16 Single-stranded oligonucleotide library (1–8) and the corresponding input strands (I_1–I_3) for the Toffoli gate. The bulge-like DNAzyme structures induce strand breaks, which in turn switch on the fluorescence from F_1–F_3. Reproduced from ref. 45.

generator adds an extra bit, the so-called parity bit, to the two data bits so that the total numbers of 1's in the string to be transmitted always is even. At the receiving end, the corresponding parity checker is analyzing this string. The checker gives an alert in form of a binary 1 for the output if the received string contains an odd number of 1's, *i.e.*, if a bit has been flipped during transmission. An essential feature for the molecule-based realization of these functions is the ability of the molecule to describe a neuron-like "off–on–off" output in response to the inputs. Triad **20** is well suited to do so, using FGo–DTEo as the initial state, degenerate 380 nm UV sources as inputs, and monitoring the FGc fluorescence intensity as the output.[39] With no UV exposure (both inputs off), no emission is observed due to the non-fluorescent nature of FGo–DTEo. Applying one UV input enriches the sample in FGc–DTEo, and intense emission from FGc results, switching the output to the on-state. Note that at this point of output reading, the sample has not yet reached the photostationary state induced by 380 nm light. Instead, a transient situation is represented in which the concentration of FGc–DTEo is close to its maximum. If both UV inputs are applied, the sample is approaching the photostationary state where the prevailing isomer is FGc–DTEc, displaying no emission due to EnT quenching of FGc by DTEc (see Section 5 for a more detailed description of the fluorescence properties of all four isomeric forms). Hence, all the requirements for the "off–on–off"-response of the fluorescence output with respect to the degenerate UV inputs are fulfilled, completing the function of the parity generator. The full operation of the parity checker is somewhat more complex and requires a combination of UV- and visible light to be used as the set of inputs.

So far in this Review, little attention has been given to molecular mimics of the keypad lock. As mentioned above, and described in our previous tutorial review,[4] this sequential logic device has been devised by numerous groups. An excellent "out-of-the-box" example that deserves special mentioning, however, is the combinatorial fluorescent molecular sensor reported by Margulies and co-workers (**22** in Fig. 17).[47,48] Rather than introducing receptors that are specific to the input analytes, this construct bears three equivalent, non-specific boronic acid receptors together with four individual fluorescence reporter groups (naphthalene, fluorene, dansyl, and anthracene). The fluorescent reporter groups have their respective emission spectrum centered on the wavelengths indicated in Fig. 17, and the overall sum-spectrum constitutes the output reading. Saccharides of various kinds together with Dabcyl catechol were used as inputs. The ability of this construct to discriminate between the different input combinations (and the sequence of application) arises from the tendency of the boronic acids to form multivalent and kinetically stable complexes with the input analytes. Due to the input-dependent structural variations of these complexes, the relative distances and orientations between the appended fluorophores change substantially, which implies that excited state intramolecular processes (*e.g.*, EnT and PET processes) are altered with the inputs. Hence, by monitoring the overall emission from the fluorescent reporters, distinct input-dependent patterns are generated that can be further treated by principal component analysis. This approach allows not only for discrimination between different input application sequences, but also between different concentrations of the inputs. This implies that the input combinations 112 and 122, where 1 and 2

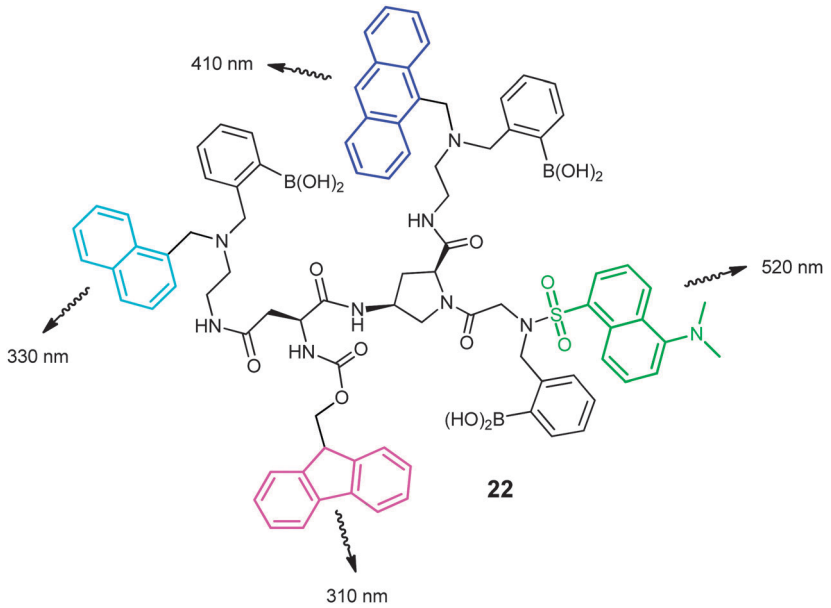

Fig. 17 The unimolecular keypad lock with three boronic acid receptors and four individual fluorophores.

denote inputs 1 and 2, generate distinguishable spectral responses (outputs), adding another dimension to the set of useful input combinations. Finally, the output reading is based on spectral pattern recognition over a broad wavelength region (rather than binary intensity values at a specific wavelength). Hence, the system can authorize and identify multiple users, each with a unique spectral pattern as an authorized output.

Magri *et al.* recently reported a multi-analyte molecular sensor, using the conventional approach, *i.e.*, by the introduction of orthogonal detection sites (**23** in Fig. 18).[49] In terms of logic gates, the sensor describes the function of a three-input AND gate with fluorescence output, which itself is not without precedence. What lends exclusiveness to this molecular construct is instead the ability to monitor the biologically and environmentally relevant properties of saltiness, pH, and pE ($[Na^+]$, $[H^+]$, and $[Fe^{3+}]$), *i.e.*, the system is to be regarded as a Na^+-enabled Pourbaix sensor. Simultaneous "turn-on" fluorescence detection of $[Na^+]$ and $[H^+]$ was demonstrated already in 1993.[2] Detection of $[Fe^{3+}]$, however, is much more complicated to achieve by this approach, as $[Fe^{3+}]$ typically quenches excited states rather than enhancing the emissive properties of fluorophores. Here, this obstacle was surmounted by using $[Fe^{3+}]$ as an oxidant, as opposed to a quenching analyte. The classical format of an anthracene-based fluorescence reporter covalently linked to a crown ether and an amino function (Na^+ and H^+ receptor, respectively) was accordingly equipped with an additional ferrocene unit. Ferrocene quenches the anthracene emission by PET, whereas this pathway is arrested upon ferrocene oxidation by, *e.g.*, Fe^{3+}. Thus, in the absence of inputs, the anthracene fluorescence is quenched by three efficient PET-processes. This implies that intense emission will be observed only in the simultaneous presence of the three cations, efficiently blocking the PET quenching channels, which is the precondition for a sensor of this kind.

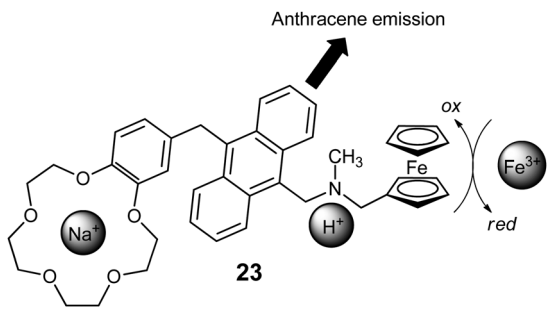

Fig. 18 Three-input AND gate for sensing of Na^+, pH, and pE.

In the vast majority of the examples highlighted above, the inputs and the outputs are described as being either "off" (0) or "on" (1), and the truth tables are constructed accordingly (truth values of 0 and 1). For many logic situations, this description is insufficient and the concept of fuzzy logic is instead applied. Here, the truth value can vary in the range between 0 and 1, which means that the concentration of a chemical species used as an input could, for example, be described as being low, medium, high, or very high. Gentili used a photochromic spirooxazine derivative (SpO) as the molecular platform, together with H^+, Al^{3+}, and Cu^{2+} as the inputs, adopting the concentration regimes mentioned above as the Fuzzy sets.[50] The addition of various input combinations to a solution of SpO followed by UV exposure to trigger the isomerization to the merocyanine (MC) form yields photostationary states [MC]/[SpO] that depend on the applied inputs. Moreover, the spectral positions of the absorption bands in the visible region shift with the input combinations, as a result of the formation of MC–H^+, MC–Al^{3+}, and MC–Cu^{2+}. As the concentrations of the inputs are allowed to vary freely, the solution can acquire an infinite number of colors, or transmission spectra. To defuzzify

this situation, the transmission spectra are partitioned in three Fuzzy sets, namely the three CIE color matching functions. The resulting coordinates are easily transformed into RGB values, which imply that each input-dependent solution/spectra has been categorized in terms of its ''redness'', ''greenness'', and ''blueness'' by crisp numbers. Depending on the relative magnitude of the *R*, *G*, and *B* values, a set of logic rules is used to describe the color of the solutions. For example, ''IF $[Cu^{2+}]$/[SpO] is High AND $[H^{+}]$/[SpO] is null, THEN the solution is Red-Green''.

7. Conclusions

A suitable way to conclude this progress report on molecular logic is to contrast it to the conclusions drawn in our previous tutorial review from 2010.[4] There, the concatenation issue was mentioned as a difficult challenge waiting ahead. It is clear from the reported advances that this obstacle has been tackled by several research groups at the level of proof-of-principle by the use of clever means for gate-to-gate communication through chemical species or energy transfer. Translation of the molecular devices from solution to surfaces was mentioned as another precondition for practical devices. Although the main part of the studies is still done in bulk solution, it is encouraging to note that examples of surface-based designs are getting more and more frequent. As for the advanced combinational and sequential logic operations performed by molecules, a number of new devices are added to the list, such as several flip-flops and conceptually novel keypad locks, three-input reversible logic gates (Toffoli and Fredkin), and parity generators/checkers. The degree of functional integration has increased dramatically, and today's most sophisticated molecular platform is able to mimic no less than 14 logic functions.

Furthermore, very interesting molecular variants that emulate the function of transistors were reported, demonstrating that conventional electronics continues to be the role model of molecular logic. The ongoing interest in the field has received a strong backup from the demonstrated application potential of molecular logic in multi-analyte detection, theranostics, the design of smart materials, and from inherently bio-inspired approaches such as the discussed enzymatic logic devices. It is expected that these results will serve as a catalyst for increasing the awareness of the conceptual molecular logic approach.

With regard to future challenges in this exciting field, the following directions are identified:

- intensify research on devices that are supported on solids and that can be addressed remotely by light or electrochemical signals,
- explore the possibilities of further increased levels of functional integration in self-assembled multichromophoric systems,
- demonstrate concatenation cascades in supramolecular assemblies of multiple logic devices,
- improve the recycling and reset capabilities of existing logic switches,
- demonstrate photonically and/or chemically driven logic operations in ''uncommon environments'', such as biological tissues and cells, leading for example, to intelligent fluorescence tags or sensors,
- further extend the principles of logic to applications, such as switchable catalysis, biomolecular recognition, or theranostics.

This list is naturally far from being complete and as recent years in this field has shown, only limited by the creativity of its authors and those who wish to join.

Acknowledgements

We thank the Swedish Research Council VR (grant 622-2010-280 for J.A.), the European Research Council (ERC FP7/2007-2013 grant No. 203952 for J.A.), the Junta de Andalucía (grant P12-FQM-2140 for U.P.), and the Spanish Ministry of Economy and Competitiveness (grant CTQ2011-28390 for U.P.) for generous financial support.

Notes and references

1 A. Aviram, *J. Am. Chem. Soc.*, 1988, **110**, 5687–5692.
2 A. P. de Silva, H. Q. N. Gunaratne and C. P. McCoy, *Nature*, 1993, **364**, 42–44.
3 K. Szaciłowski, *Chem. Rev.*, 2008, **108**, 3481–3548.
4 J. Andréasson and U. Pischel, *Chem. Soc. Rev.*, 2010, **39**, 174–188.
5 A. P. de Silva, *Molecular Logic-based Computation*, The Royal Society of Chemistry, Cambridge, 2013.
6 T. Miyamoto, S. Razavi, R. DeRose and T. Inoue, *ACS Synth. Biol.*, 2013, **2**, 72–82.
7 U. Pischel, J. Andréasson, D. Gust and V. F. Pais, *ChemPhysChem*, 2013, **14**, 28–46.
8 J. Andréasson, U. Pischel, S. D. Straight, T. A. Moore, A. L. Moore and D. Gust, *J. Am. Chem. Soc.*, 2011, **133**, 11641–11648.
9 T. Niazov, R. Baron, E. Katz, O. Lioubashevski and I. Willner, *Proc. Natl. Acad. Sci. U. S. A.*, 2006, **103**, 17160–17163.
10 S. Erbas-Cakmak and E. U. Akkaya, *Angew. Chem., Int. Ed.*, 2013, **52**, 11364–11368.
11 S. Ozlem and E. U. Akkaya, *J. Am. Chem. Soc.*, 2009, **131**, 48–49.
12 S. Erbas-Cakmak, O. A. Bozdemir, Y. Cakmak and E. U. Akkaya, *Chem. Sci.*, 2013, **4**, 858–862.
13 S. Pramanik, S. De and M. Schmittel, *Angew. Chem., Int. Ed.*, 2014, **53**, 4709–4713.
14 S. Pramanik, S. De and M. Schmittel, *Chem. Commun.*, 2014, **50**, 13254–13257.
15 D. Ray, J. T. Foy, R. P. Hughes and I. Aprahamian, *Nat. Chem.*, 2012, **4**, 757–762.
16 S. Silvi, A. Arduini, A. Pochini, A. Secchi, M. Tomasulo, F. M. Raymo, M. Baroncini and A. Credi, *J. Am. Chem. Soc.*, 2007, **129**, 13378–13379.
17 S. Silvi, E. C. Constable, C. E. Housecroft, J. E. Beves, E. L. Dunphy, M. Tomasulo, F. M. Raymo and A. Credi, *Chem. – Eur. J.*, 2009, **15**, 178–185.

18 R. Guliyev, S. Ozturk, Z. Kostereli and E. U. Akkaya, *Angew. Chem., Int. Ed.*, 2011, **50**, 9826–9831.
19 E. Tanriverdi Ecik, A. Atilgan, R. Guliyev, T. B. Uyar, A. Gumus and E. U. Akkaya, *Dalton Trans.*, 2014, **43**, 67–70.
20 M. Elstner, J. Axthelm and A. Schiller, *Angew. Chem., Int. Ed.*, 2014, **53**, 7339–7343.
21 M. Elstner, K. Weisshart, K. Müllen and A. Schiller, *J. Am. Chem. Soc.*, 2012, **134**, 8098–8100.
22 U. Pischel and J. Andréasson, *New J. Chem.*, 2010, **34**, 2701–2703.
23 R. Baron, A. Onopriyenko, E. Katz, O. Lioubashevski, I. Willner, S. Wang and H. Tian, *Chem. Commun.*, 2006, 2147–2149.
24 G. Periyasamy, J.-P. Collin, J.-P. Sauvage, R. D. Levine and F. Remacle, *Chem. – Eur. J.*, 2009, **15**, 1310–1313.
25 G. de Ruiter, E. Tartakovsky, N. Oded and M. E. van der Boom, *Angew. Chem., Int. Ed.*, 2010, **49**, 169–172.
26 G. de Ruiter, L. Motiei, J. Choudhury, N. Oded and M. E. van der Boom, *Angew. Chem., Int. Ed.*, 2010, **49**, 4780–4783.
27 R. Ferreira, P. Remón and U. Pischel, *J. Phys. Chem. C*, 2009, **113**, 5805–5811.
28 V. F. Pais, P. Remón, D. Collado, J. Andréasson, E. Pérez-Inestrosa and U. Pischel, *Org. Lett.*, 2011, **13**, 5572–5575.
29 T. Avellini, H. Li, A. Coskun, G. Barin, A. Trabolsi, A. N. Basuray, S. K. Dey, A. Credi, S. Silvi, J. F. Stoddart and M. Venturi, *Angew. Chem., Int. Ed.*, 2012, **51**, 1611–1615.
30 P. Remón, M. Bälter, S. M. Li, J. Andréasson and U. Pischel, *J. Am. Chem. Soc.*, 2011, **133**, 20742–20745.
31 P. Remón, M. Hammarson, S. M. Li, A. Kahnt, U. Pischel and J. Andréasson, *Chem. – Eur. J.*, 2011, **17**, 6492–6500.
32 Q. Zou, X. Li, J. J. Zhang, J. Zhou, B. B. Sun and H. Tian, *Chem. Commun.*, 2012, **48**, 2095–2097.
33 Y. Wu, Y. S. Xie, Q. Zhang, H. Tian, W. H. Zhu and A. D. Q. Li, *Angew. Chem., Int. Ed.*, 2014, **53**, 2090–2094.
34 K. MacVittie, J. Halámek, V. Privman and E. Katz, *Chem. Commun.*, 2013, **49**, 6962–6964.
35 A. J. M. Huxley, M. Schroeder, H. Q. N. Gunaratne and A. P. de Silva, *Angew. Chem., Int. Ed.*, 2014, **53**, 3622–3625.
36 M. Shaikh, J. Mohanty, A. C. Bhasikuttan, V. D. Uzunova, W. M. Nau and H. Pal, *Chem. Commun.*, 2008, 3681–3683.
37 A. E. Keirstead, J. W. Bridgewater, Y. Terazono, G. Kodis, S. Straight, P. A. Liddell, A. L. Moore, T. A. Moore and D. Gust, *J. Am. Chem. Soc.*, 2010, **132**, 6588–6595.
38 M. Pärs, C. C. Hofmann, K. Willinger, P. Bauer, M. Thelakkat and J. Köhler, *Angew. Chem., Int. Ed.*, 2011, **50**, 11405–11408.
39 M. Bälter, S. M. Li, J. R. Nilsson, J. Andréasson and U. Pischel, *J. Am. Chem. Soc.*, 2013, **135**, 10230–10233.
40 D. Gust, J. Andréasson, U. Pischel, T. A. Moore and A. L. Moore, *Chem. Commun.*, 2012, **48**, 1947–1957.
41 S. J. Chen, Y. H. Yang, Y. Wu, H. Tian and W. H. Zhu, *J. Mater. Chem.*, 2012, **22**, 5486–5494.
42 G. de Ruiter and M. E. van der Boom, *Angew. Chem., Int. Ed.*, 2012, **51**, 8598–8601.
43 M. Semeraro and A. Credi, *J. Phys. Chem. C*, 2010, **114**, 3209–3214.
44 P. Remón, R. Ferreira, J. M. Montenegro, R. Suau, E. Pérez-Inestrosa and U. Pischel, *ChemPhysChem*, 2009, **10**, 2004–2007.
45 R. Orbach, F. Remacle, R. D. Levine and I. Willner, *Proc. Natl. Acad. Sci. U. S. A.*, 2012, **109**, 21228–21233.
46 R. Orbach, F. Remacle, R. D. Levine and I. Willner, *Chem. Sci.*, 2014, **5**, 1074–1081.
47 B. Rout, L. Unger, G. Armony, M. A. Iron and D. Margulies, *Angew. Chem., Int. Ed.*, 2012, **51**, 12477–12481.
48 B. Rout, P. Milko, M. A. Iron, L. Motiei and D. Margulies, *J. Am. Chem. Soc.*, 2013, **135**, 15330–15333.
49 D. C. Magri, M. C. Fava and C. J. Mallia, *Chem. Commun.*, 2014, **50**, 1009–1011.
50 P. L. Gentili, *Phys. Chem. Chem. Phys.*, 2011, **13**, 20335–20344.